Energy Conversion and Management 138 (2017) 486–492

Contents lists available at ScienceDirect

Energy Conversion and Management

journal homepage: www.elsevier.com/locate/enconman

Experimental investigation on the thermal performance of heat pipe-assisted phase change material based battery thermal management system

Weixiong Wu [a], Xiaoqing Yang [b], Guoqing Zhang [b], Kai Chen [a], Shuangfeng Wang [a,*]

[a] Key Laboratory of Enhanced Heat Transfer & Energy Conservation, Ministry of Education, South China University of Technology, Guangzhou 510640, Guangdong, China
[b] School of Material and Energy, Guangdong University of Technology, Guangzhou 510006, Guangdong, China

ARTICLE INFO

Article history:
Received 23 December 2016
Received in revised form 8 February 2017
Accepted 9 February 2017
Available online 21 February 2017

Keywords:
Phase change material
Heat pipe
Thermal performance
Battery thermal management

ABSTRACT

In this paper, a heat pipe-assisted phase change material (PCM) based battery thermal management (BTM) system is designed to fulfill the comprehensive energy utilization for electric vehicles and hybrid electric vehicles. Combining the large heat storage capacity of the PCM with the excellent cooling effect of heat pipe, the as-constructed heat pipe-assisted PCM based BTM is feasible and effective with a relatively longer operation time and more suitable temperature. The experimental results show that the temperature maldistribution of battery module can be influenced by heat pipes when they are activated under high discharge rates of the batteries. Moreover, with forced air convection, the highest temperature could be controlled below 50 °C even under the highest discharge rate of 5C and a more stable and lower temperature fluctuation is obtained under cycling conditions. Meanwhile, the effectiveness of further increasing air velocity (i.e., more fan power consumption) is limited when the highest temperature continues to reduce at a lower rate due to the phase transition process of PCM. These results are expected to provide insights into the design and optimization of BTM systems.

1. Introduction

Under the mounting pressure of emissions legislation and energy shortage, pure electric vehicles (EVs) and hybrid electric vehicles (HEVs) with highly efficient drive systems and green energy power are viable alternatives to conventional vehicles with combustion engines. Secondary Li-ion batteries are normally used as the power source for EVs and HEVs because of their good stability, high voltage, low self-discharge rate and high energy density [1,2]. Nevertheless, both extreme environmental and operating temperatures will affect the reliability, lifespan and safety of the batteries. The temperatures of all cells must be maintained within an operating range between 20 °C and 50 °C for the tolerable operation [3]. Cells are vulnerable to overheating from rapid discharging, overcharging or excessive ambient heating. Such issues can lead to rapid cell degradation and shorten battery life. Thus, an efficient and feasible battery thermal management (BTM) system for EVs and HEVs is essential to control the operating temperature of batteries within an appropriate range.

Consequent to these requirements, considerable research efforts have been invested to develop an advanced BTM system which can be summarized as several types based on the employment of different heat transfer medium such as air [4], liquid [5,6] and phase change material based systems and combination of them [7]. As an innovative solution for thermal management applications, PCM can absorb/release abundant latent heat during the melting/solidifying process, giving rise to a relatively constant temperature for the PCM based system, which make this type of BTM system receive extensive attention and exploration in recent years [8]. The thermal management solution using PCM as heat transfer medium was first proposed by Al-Hallaj and Selman [9] in 2000, in which the paraffin mixture was used as the PCM and filled in the gap between batteries. The as-designed PCM based BTM system actually showed a much better thermal performance than conventional systems.

Currently, paraffin wax is the most widely researched PCM for BTM because of its low cost, hard-to-decompose character and a broad range of suitable phase-change temperature varying with the number of main chain carbon atoms [7]. Unfortunately, one of the main bottlenecks that limits the application of PCM is its low thermal conductivity. In regard to this weakness, many different approaches have been developed to enhance the thermal

* Corresponding author.
E-mail address: sfwang@scut.edu.cn (S. Wang).

http://dx.doi.org/10.1016/j.enconman.2017.02.022
0196-8904/

Nomenclature

T	temperature (°C)
ΔT	temperature difference (°C)
Acronyms	
PCM	phase change material
EG	expanded graphite
EVs	pure electric vehicles
HEVs	hybrid electric vehicles
BTM	battery thermal management
HP	heat pipe
OHP	oscillating heat pipe
PCMP	phase change material plate

conductivity of PCM by introducing a second component made of high conductive materials such as metallic particle [10], metal foam/mesh [11,12], carbon fiber [13], graphene [14,15] and carbon nanotubes [16]. Al-Hallaj et al. [17] designed different modes of heat dissipation for Li-ion battery modules and tested at various constant C-rates, the results showed that the distribution of PCM in the pores of aluminum foam resulted in a minor temperature drop when compared to PCM alone and a significant drop of about 50% compared to natural convection cooling. Under the road operating state, that is, the fluctuations of discharge current, such paraffin/metal foam technology is also efficient for BTM within EVs [18]. However, closed tanks or containers are necessary to prevent leakage of liquid-phase PCM when the temperature of the PCM is over the melting point, giving rise to a relatively complex structure in practical applications.

Expanded graphite (EG) material as a porous matrix is often inserted into PCMs due to its high thermal conductivity (about 200 $W\ m^{-1}\ K^{-1}$) and high porosity for increasing absorbability, which is favorable for the creation of thermal conductive networks within the composite PCM and shape-stabilized during the solid-liquid phase change [19,20]. With EG impregnated in the PCM, the total thermal conductivity of composite PCM was increased by two orders of magnitude and the performance of the BTM system was significantly improved in comparison to the original battery packs [21,22]. The thermo mechanical properties of PCM/EG composites such as tensile strength, burst strength, compression strength and bending strength were also studied in Refs. [23,24]. Wu et al. [25] proposed a copper mesh-enhanced PCM/EG composite BTM for prismatic batteries, in which the as-constructed system presented much better heat dissipation performance and temperature uniformity compared to PCM/EG based system. In spite of the high efficiency, the PCM/EG based system without any other cooling methods still encountered the problem that single PCM-based cooling technology usually presents low surface heat transfer coefficient between PCM and air, which may lead to the running out of the available latent heat under extreme conditions [25,26].

Heat Pipe (HP), as a high efficient heat transfer device with excellent characteristics such as compact structure, flexible geometry and long service life, has been widely used in thermal energy storage system [27,28] and electronic thermal management [29]. In the latent heat storage system, the assisted HP can amplify the charging/discharging process rate of PCM and thus improve the overall thermal performance [30–32]. For the usage on battery, HP based BTM systems were fully studied experimentally [33–39] and theoretically/numerically [40–42]. Wu et al. [43] proposed a method by applying HP with aluminum fins in a Li-ion battery pack and it was found that HP cooling is an effective method which can reduce the temperature rise and maintain a uniform temperature distribution over the battery surface. On account of the excellent advantages in simple design and cooling performance of oscillating heat pipe (OHP), an OHP-cooled simulative batteries system was designed and experimentally studied by Rao [44]. Further, considering the large heat storage capacity of the PCM, some changes were made and paraffin as PCM was added into the simulative OHP cooling system [45]. They concluded that some methods should be taken to increase the thermal conductivity of paraffin for the purpose of further improving the thermal performance of the BTM systems. Moreover, by taking into account the literature survey, it can be noted that the performance of HP/PCM coupled system has not been experimentally studied for real batteries, especially based on module level. In addition, a feasible and effective system with the feature of easy package is essential and should be further explored due to the potential for practical application.

In our previous work [46], a kind of shape-stabilized PCM/EG composite plate with enhanced thermal conductivity was prepared for use in the field of thermal management and this method can be also used in various practical applications. In order to further optimize the thermal performance of BTM system, a HP-assisted PCM/EG composite plate based BTM system was designed for EVs and HEVs in this study. Sub-modules were fabricated and then investigated experimentally under different operating conditions. As highlighted here, paraffin with large latent heat serves as the thermal buffer. Porous EG with high thermal conductivity can create thermal conductive networks and absorb liquid phase paraffin to address the leakage problem. HP acts as a heat conductor to further increase the heat absorption rate of PCM/EG composite, and also extract the heat from battery module to the external air environment. The as-designed battery pack with the feature of easy package is expected to be enclosed, leaving only a channel for heat exchange at side of the battery box, to meet the compact and water/moisture-seal requirements for practical applications.

2. Concept description

For EVs and HEVs applications, a compact and well designed battery pack is necessary because of the limited space in EVs and HEVs. Fig. 1 shows a generic design of pack-scale BTM system, in which there are several sub-modules in series/parallel arrangement. In the design, the battery pack consists of PCM composites surrounding the array of battery monomers. The evaporating section of HP is integrated within PCM with the condenser end extending outside of the battery box. An air flow channel on the side of the battery pack serves as the heat exchanger, where air could be blown through the finned condenser using fans. Such a novel thermal management system is designed to be compact and efficient.

Before constructing a commercial scale battery pack, a lab-scale battery module is usually used firstly to confirm the feasibility of a new thermal management strategy. A sub-module consisted of five commercially prismatic batteries (3.2 V/12 A h) in series connection rated at 16 V/12 A h was used as the research object in this work. In this module, six phase change material plates (PCMPs) with a thickness of 5 mm and five batteries were stacked alternately to form a compact sandwich structure. Two HP-assisted PCMPs were in contact with both long sides of this module. A typical HP-assisted PCMP (HP-PCMP) can be also seen in Fig. 1.

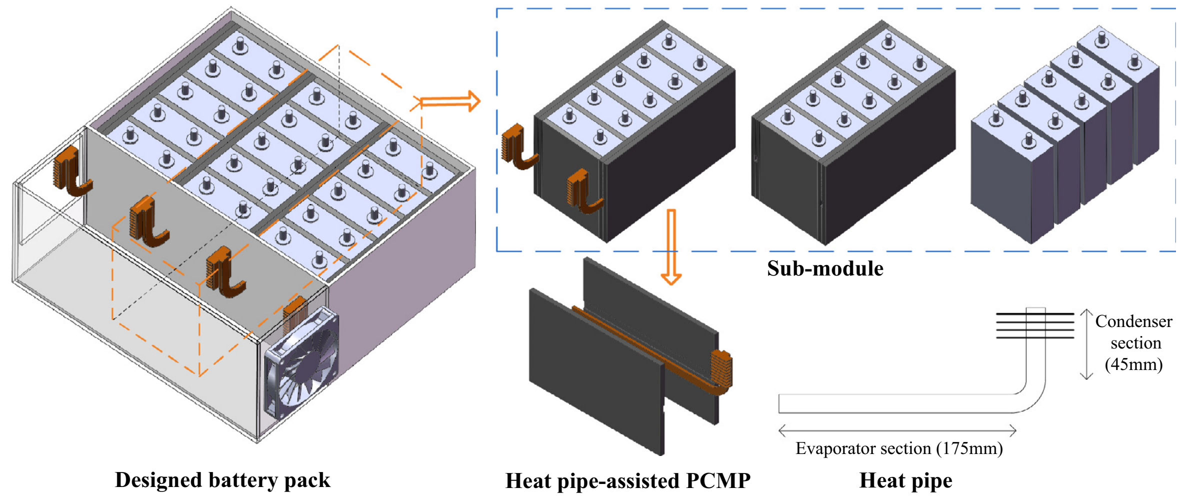

Fig. 1. Schematic illustrations of designed battery pack and sub-modules.

Each L-shape HP was sandwiched between two PCMPs and embedded in the corresponding grooves milled on the surface of PCMPs. Thermal grease was applied at the interfaces between the evaporation section of HP and PCMP as well as the battery and PCMP. The L-shape HP (sintered copper-water) used here is flattened, and the width and thickness are 8 mm and 3 mm, respectively. The HP has an evaporator section with 175 mm in length and a condensation section with 45 mm in length (Fig. 1).

During the operation, the heat generated within the cells is absorbed by PCM and then conducted through the evaporating section of the HP to the condenser section. The heat transfer and exchange process of this module is illustrated in Fig. 2, there are mainly two areas for this process: (1) The PCM absorbs and stores heat generated within cells by utilizing sensible heat or latent heat during phase change, and (2) assisted HP enhances the heat absorption rate of PCM and the heat dissipation capacity from module to the external air environment. Thus, to achieve the heat transportation and the decrease of battery temperature, PCMP with relatively high thermal conductivity and condenser section of HP with requested heat exchange capacity are expected to increase the thermal performance of the overall module. Details of the preparation and thermal characteristics of PCMP were reported by our previous study [46] and the related thermo-physical parameters are listed in Table 1. It shows that the thermal conductivity of composite PCM is about 30 times higher than that of pure paraffin owing to the addition of EG that has a high thermal conductivity. On the other hand, a finned array is soldered to the condenser section of HP, and from there heat is removed by forced air convection to further enhance the cooling performance.

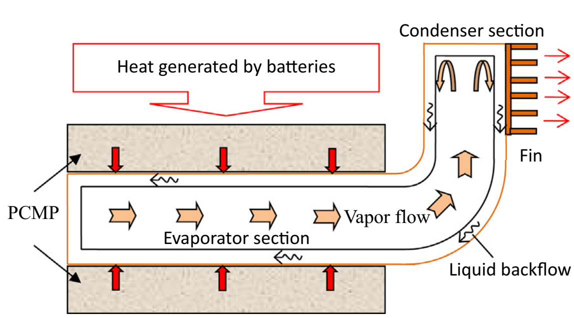

Fig. 2. Schematic diagram of heat transfer in HP-PCMP module.

Table 1
Thermo-physical parameters.

	Melting point (°C)	Thermal conductivity (W m^{-1} K^{-1})	Latent heat (J g^{-1})
Paraffin	42.02	0.268	186.4
Paraffin/EG	41.71	7.654	141.7

3. Experimental setup

The schematic diagram of experimental setup is shown in Fig. 3. A battery testing system (BTS-50V120A-NTF, Shenzhen Neware Electronics Co. Ltd, China) with an accuracy of ±0.01% was used to charge and discharge the battery module. T-type thermocouples (omega type TT-T-30-SLE-1M, accuracy of ±0.1 °C) were attached to the surface center of each battery for recording the temperature by a PC-based data acquisition unit (Agilent 34970A). All thermocouples were calibrated in the temperature range of 0–100 °C with a standard thermometer. A fan was used to blow the air through the finned array to form forced air convection. The velocity of flowing air through the condenser section of HP was measured and controlled by an anemograph and AC power supply, respectively. The voltage and current indicated by the AC power supply were verified with a standard calibrated multi-meter and the uncertainties in the voltage and current measurements were ±0.1 V and ±0.01 A, respectively. The evaluation of uncertainties can be calculated as $\Delta\sigma = \pm\sqrt{\sum_{i=1}^{N}\left(\frac{\partial\sigma}{\partial m_i}\times\Delta m_i\right)^2}$ based on the uncertainty of primary quantities [47], thus the resulting uncertainty of temperature was estimated to be within ±0.5%. During the experiments, charge and discharge procedures (Table 2) were performed for the battery modules. For comparison, another two battery modules with and without PCMP were also assembled with a similar configuration.

4. Results and discussions

4.1. Temperature control

Fig. 4 shows the maximum temperature (T_{max}) variations for the modules of the No PCM, the PCMP and the HP-PCMP under the condition of natural convection with different discharge rates (1C, 3C, 5C). During the 1C discharge process, as seen in Fig. 4(a), the temperatures for the three modules increase in a similar

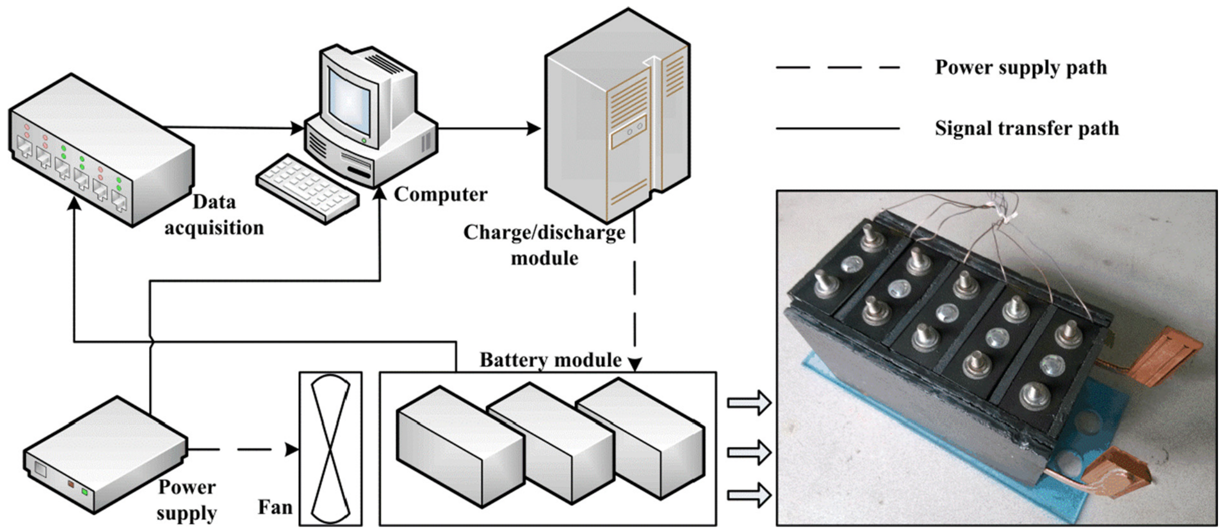

Fig. 3. Sketch of the experimental system and battery module with HP-PCMP.

Table 2
Charge/discharge procedures.

Process		Current (A)	Voltage (V)
Charge	Galvanostatic	12 (1C)	Cut-off voltage of 18.25
	Potentiostatic	Cut-off current of 1.8	18.25
Discharge	–	12–60 (1–5C)	Cut-off voltage of 12.5

manner and the highest temperatures are all below 30 °C. This result indicates that the paraffin within PCMP still remains solid phase and the HP is not started yet during the discharge rate of 1C, which leads to the conclusion that thermal conduction is the dominant heat transfer mechanism. However, the temperatures of PCMP and HP-PCMP are slightly less than that of the No PCM module, which can be attributed to the high thermal conductivity of the EG (*c.a.* ~200 $W\ m^{-1}\ K^{-1}$) and assisted HP.

As for 3C discharge rate depicted in Fig. 4(b), a significant decrease of the heating rate is observed in PCMP and HP-PCMP module because phase transition occur to store thermal energy as latent heat of fusion at a temperature range corresponding to the melting point of paraffin. In addition, the HP-PCMP module gets the best performing temperature rising with the function of assisted HP as the temperature of the evaporation section reached the started-up temperature. As a result, the highest temperature for No PCM, PCMP and HP-PCMP is 47.8 °C, 44.1 °C and 42.8 °C, respectively.

For the modules undergoing a 5C discharge rate, the T_{max} profiles are shown in Fig. 4(c). The temperature for No PCM module is much higher than the other two modules, and a highest temperature of 63.1 °C is obtained in the absence of PCMP and HP, which exceeds the point of 50 °C by almost 13 °C. Comparatively, the highest temperature of the module with PCMP is 53.2 °C, almost 10 °C lower than the former. When HP is introduced to PCMP, the absorbed heat in paraffin near the evaporation side can be exported through the HP. So the highest temperature is further decreased to 50.9 °C, very close to the recommended upper operation temperature of 50 °C during such a high discharge rate. The time to reach a set point temperature of 50 °C for No PCM, PCMP and HP-PCMP is 488 s, 640 s, and 701 s, respectively. These results indicate that the as-constructed HP-PCMP module is more suitable in BTM especially during high discharge rate, because it offers a relatively longer operation time and more suitable temperature.

4.2. Temperature distribution

The temperature distributions of the three modules at the end of different discharge rates (1C, 3C, 5C) are shown in Fig. 5. A maximum temperature at the center and a minimum temperature at the corner are observed for all three modules due to the different heat dissipation conditions. However, the temperature region near the condenser side of HP has the tendency of decreasing compared to that of No PCM and PCMP modules under the high discharge rates of 3C and 5C. In these stages, the HP is activated and the backflow of working fluid in the part of the evaporator closed to the condenser side can be more easily evaporated and transported to the condensation section. Therefore, the structural design optimization of HP assisted BTM system should be taken into account for the purpose of further achieving a well-designed scale-up battery pack.

The temperature difference (ΔT) in the module is a main index to evaluate the thermal performance of BTM, which is given by:

$$\Delta T = T_{max} - T_{min}$$

where T_{max} and T_{min} represent the maximum and minimum temperature of batteries in the module. Fig. 6 shows the maximum ΔT in the modules at the end of different discharge rates. A lager ΔT can be observed with the increase of discharge rates. For the module integrated with PCMP or HP-PCMP, the ΔT is obviously decreased compared with the No PCM module at the same discharge rate. The main reason is that the heat of the center battery can be timely conducted along the long side direction of the module due to the high thermal conductivity of PCMP and assisted HP, while the No PCM module can only transfer the heat through natural air convection. As a result, a lower ΔT (a decreased rate of ~21%) of HP-PCMP than that of No PCM during the 5C rate is obtained (2.0 °C *vs.* 2.6 °C), implying the excellent thermal performance of the as-constructed HP assisted module from another point of view. Considering the criterion of 5 °C for the module temperature difference, such an extra improvement is acceptable.

4.3. Effect of forced air flow

The comprehensive performance of power battery is highly influenced by the increasing of temperature. A highest temperature above 50 °C is observed for HP-PCMP at 5C discharge rate in Section 4.1. Such a situation may lower the longevity properties

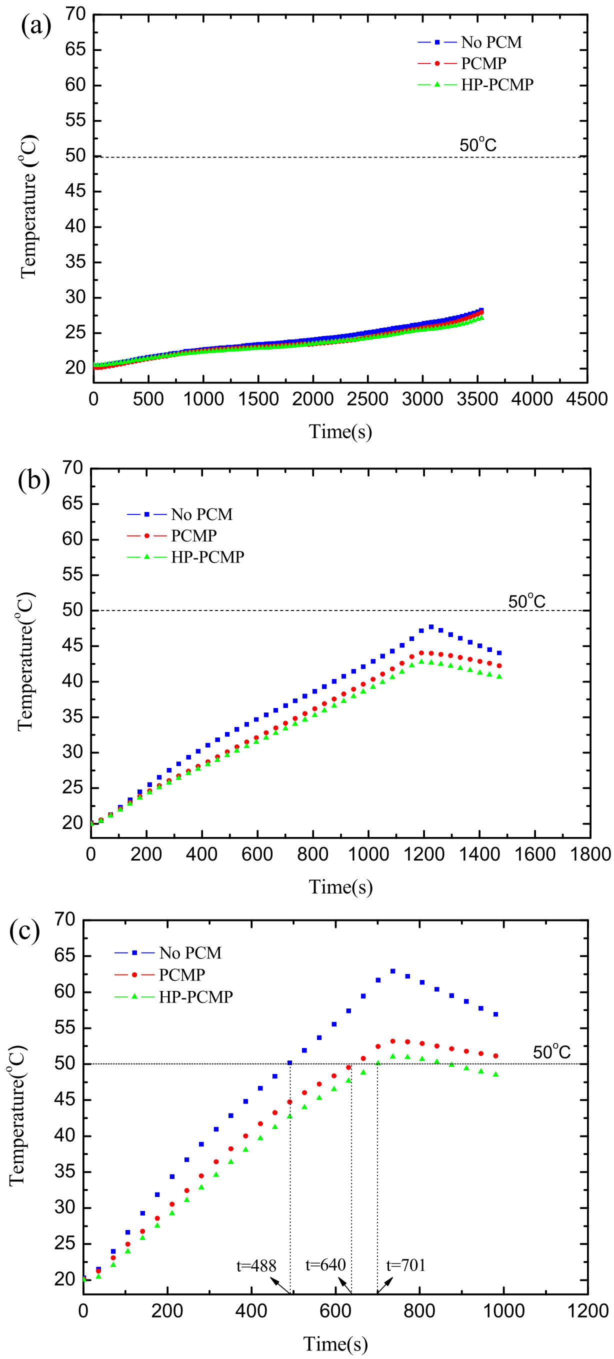

Fig. 4. Temperature response of three modules under different discharge rates: (a) 1C; (b) 3C and (c) 5C.

or the discharging efficiency of power batteries. Therefore, it is speculated that combining the condenser section with forced air flow will improve the heat transfer capability, thus further decreasing the highest temperature. In order to verify the cooling effect, the air flow velocity was set directly from 1 m s^{-1} to 4 m s^{-1}, and the temperature profiles of the HP assisted module for the 5C discharge rate are shown in Fig. 7. It is observed that the highest temperature decreases with the increasing of air flow velocity and can be controlled lower than 50 °C. For example, when the air flow velocity increases to 1 m s^{-1}, the highest temperature is decreased from 50.9 °C to 49.4 °C. However, when further increasing the flowing air velocity, the highest temperature continues to reduce at a lower rate due to the phase transition process of

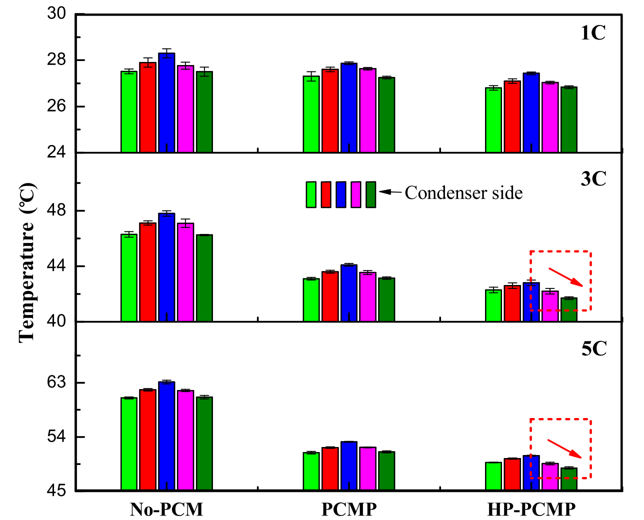

Fig. 5. Temperature distribution of three modules at the end of different discharge rates.

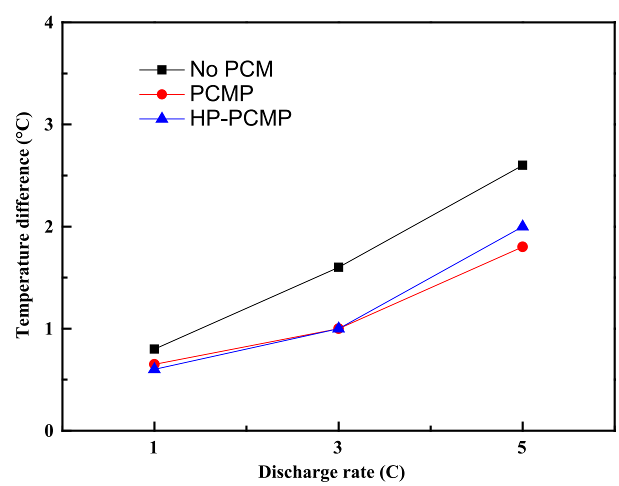

Fig. 6. Maximum temperature difference of three modules at the end of different discharge rates.

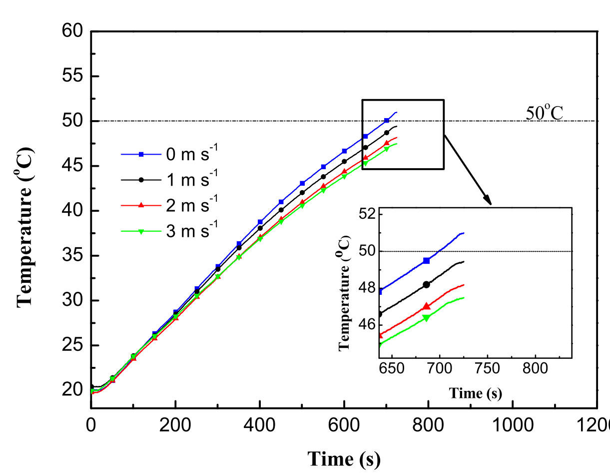

Fig. 7. Temperature variations of the HP-PCMP module under different air velocity at 5C discharge process.

PCM. In this process, the temperature of evaporating section of HP remains constant. The effectiveness of further increasing velocity is limited when the velocity reaches a critical value. Thus, a higher velocity (i.e., more fan power consumption) over the critical value is expected to be undesirable.

4.4. Cycle test

In real life driving conditions, battery power profiles are always dynamic under road operating state. To further investigate the thermal performance of the as-designed HP-PCMP technology in a practical application, cycling conditions were experimentally simulated. A testing schedule consisted of a periodic charge and discharge as shown in Fig. 8 was performed. The charging and discharging rates were 2C and 5C, respectively. It can be clearly seen in Fig. 9 that during the cycles, the initial and maximum temperature of each cycle for PCMP increase gradually, while HP-PCMP with/without forced air convection reach a stable stage (same temperature profile with previous cycle) after the first cycle. During the first discharge process, the thermal energy is stored with utilization of the latent heat in the PCM. If the absorbed heat cannot be transported to the outer air environment promptly due to the poor heat transfer efficiency, the whole battery module will undergo a higher temperature and resulting in a different starting temperature during next cycle. As a result, the initial temperature of PCMP module is 20.0 °C, 36.8 °C, 41.1 °C and 42.4 °C at the first, second, third and fourth cycle, respectively, giving rise to an increasing maximum temperature of each discharge process (53.2 °C, 60.7 °C, 63.3 °C and 63.7 °C, respectively). Therefore, the battery module which is expected to be with the suitable temperature operating limits in driving cycles cannot be achieved in the case of using PCMP alone. In the terms of HP-PCMP module, a stable initial and maximum temperature stays at about 32.9 °C and 55.7 °C is obtained after stabilization due to the enhanced effective heat transfer coefficient caused by the assisted HP. After adding a forced air flow of 3 m s^{-1}, the maximum temperature at

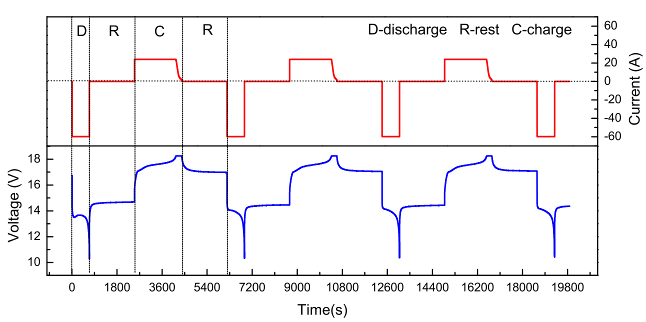

Fig. 8. Testing schedule of the current and voltage change.

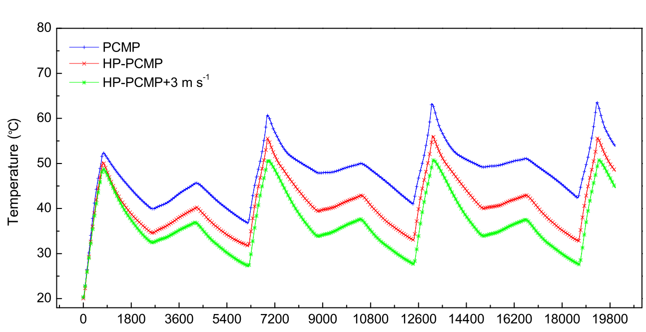

Fig. 9. Temperature variations with time for cycle test.

the steady state can be further dropped by 5.2 °C as compared with no forced air convection. These points confirm that HP-PCMP coupled with forced convection will further improve thermal performance by increasing the heat transfer capability of HP in practical applications.

4.5. Further discussions

From the material point of view, industrial paraffin and EG are considered as the most suitable materials for using as PCM and thermal conductivity skeleton in PCMP because of their low cost and high performance. For the manufacturing aspect, EG can be easily obtained from expandable graphite through a common heating method and the preparation procedure of PCMP can be simplified by developing a mold to prepare several PCMP at once. The assisted HP is for industrial use, which has been widely adopted in the field of thermal management. In short, the raw materials of HP-PCMP are all industrial available. It is technically simple for the manufacturers to change their existing process and adopt techniques in order to accomplish the task of building battery packs that include HP-PCMP. The only process that they have to change is to develop molds and battery containers with suitable sizes based on the cell geometry and quantity. The weak point that has limited the widespread use of HP is the use of copper. However, recent researches show that aluminum HP manufacturing has revealed reliable way to decrease the cost as well as the weight of the system [48].

As the processes of the decomposition and reaction in the battery are very complex, the battery power solicitation profiles are always dynamic and the generated heat is of large amplitude, which is difficult to determine. For a scale-up battery module/pack, an efficient battery management system is very important, in which the battery status determine the outputs such as cell equalization and thermal management to do the thermal control among the cells. To further facilitate vehicle-mounted energy optimization and reduce the power supply, an integrated vehicle thermal management system with appropriate energy allocation is required. Our further studies will focus on the energy allocation and delivery in HP-assisted PCM based technology.

5. Conclusions

Aiming at the BTM system for EVs and HEVs, a HP-assisted PCM based BTM system was designed to be compact and efficient from the point of practical application. Maximum temperature rise and temperature distribution within the presented battery module were experimentally studied under different discharge rates. The effects of forced air convention and cycling conditions for practical application were also analyzed. The main conclusions could be made as follow:

(1) The HP-assisted PCM based BTM system is effective and feasible for EVs and HEVs. For the use of PCM and HP, significant reduction in temperature is observed compared with no cooling strategy especially during high discharge rates. In addition, HP-PCMP module has a relatively longer operation time to reach the set point temperature of 50 °C compared to PCMP module.
(2) Temperature uniformity can be improved by using PCM. The temperature region near the condenser side of HP has the tendency of decreasing compared to that of No PCM and PCMP modules when the HP has been activated.
(3) The highest temperature can be controlled under 50 °C as forced air convention is used to enhance the heat transfer coefficient. But the effectiveness of further increasing air

velocity is limited when the velocity reaches a critical value during the phase transition process of PCM.

(4) For the case of cycle conditions, HP-PCMP module will reach a stable stage with a same temperature profile after the first cycle, while the PCMP module without HP continues to increase.

Acknowledgements

The authors appreciate the support of the National Natural Science Foundation of China (Grant No. 51536003) and the National Natural Science Foundation of China (Grant No. 51602061).

References

[1] Etacheri V, Marom R, Ran E, Salitra G, Aurbach D. Challenges in the development of advanced Li-ion batteries: a review. Energy Environ Sci 2011;4:3243–62.
[2] Qian Z, Li Y, Rao Z. Thermal performance of lithium-ion battery thermal management system by using mini-channel cooling. Energy Convers Manage 2016;126:622–31.
[3] Pesaran AA. Battery thermal models for hybrid vehicle simulations. J Power Sources 2002;110:377–82.
[4] Saw LH, Ye YH, Tay AAO, Chong WT, Kuan SH, Yew MC. Computational fluid dynamic and thermal analysis of Lithium-ion battery pack with air cooling. Appl Energy 2016;177:783–92.
[5] Huo YT, Rao ZH, Liu XJ, Zhao JT. Investigation of power battery thermal management by using mini-channel cold plate. Energy Convers Manage 2015;89:387–95.
[6] Zhao J, Rao Z, Li Y. Thermal performance of mini-channel liquid cooled cylinder based battery thermal management for cylindrical lithium-ion power battery. Energy Convers Manage 2015;103:157–65.
[7] Rao ZH, Wang SF. A review of power battery thermal energy management. Renew Sustain Energy Rev 2011;15:4554–71.
[8] Zhang P, Xiao X, Ma ZW. A review of the composite phase change materials: fabrication, characterization, mathematical modeling and application to performance enhancement. Appl Energy 2016;165:472–510.
[9] Al Hallaj S, Selman JR. A novel thermal management system for electric vehicle batteries using phase-change material. J Electrochem Soc 2000;147:3231–6.
[10] Huang C, Wang Q, Rao Z. Thermal conductivity prediction of copper hollow nanowire. Int J Therm Sci 2015;94:90–5.
[11] Li WQ, Qu ZG, He YL, Tao YB. Experimental study of a passive thermal management system for high-powered lithium ion batteries using porous metal foam saturated with phase change materials. J Power Sources 2014;255:9–15.
[12] Azizi Y, Sadrameli S. Thermal management of a $LiFePO_4$ battery pack at high temperature environment using a composite of phase change materials and aluminum wire mesh plates. Energy Convers Manage 2016;128:294–302.
[13] Azizi M, Samimi F, Babapoor A, Karimi G. Thermal management analysis of a Li-ion battery cell using phase change material loaded with carbon fibers. Energy 2016;96:355–71.
[14] Goli P, Legedza S, Dhar A, Salgado R, Renteria J, Balandin AA. Graphene-enhanced hybrid phase change materials for thermal management of Li-ion batteries. J Power Sources 2013;248:37–43.
[15] Mehrali M, Latibari ST, Rosen MA, Akhiani AR, Naghavi MS, Sadeghinezhad E, et al. From rice husk to high performance shape stabilized phase change materials for thermal energy storage. RSC Adv 2016;6:45595–604.
[16] Shirazi AHN, Mohebbi F, Kakavand MRA, He B, Rabczuk T. Paraffin nanocomposites for heat management of lithium-ion batteries: a computational investigation. J Nanomater 2016;2016:1–10.
[17] Khateeb SA, Amiruddin S, Farid M, Selman JR, Al-Hallaj S. Thermal management of Li-ion battery with phase change material for electric scooters: experimental validation. J Power Sources 2005;142:345–53.
[18] Rao Z, Huo Y, Liu X, Zhang G. Experimental investigation of battery thermal management system for electric vehicle based on paraffin/copper foam. J Energy Inst 2014;88:241–6.
[19] Wang T, Wang S, Geng L, Fang Y. Enhancement on thermal properties of paraffin/calcium carbonate phase change microcapsules with carbon network. Appl Energy 2016;179:601–8.
[20] Yan J, Li K, Chen H, Wang Q, Sun J. Experimental study on the application of phase change material in the dynamic cycling of battery pack system. Energy Convers Manage 2016;128:12–9.
[21] Mills A, Al-Hallaj S. Simulation of passive thermal management system for lithium-ion battery packs. J Power Sources 2005;141:307–15.
[22] Mills A, Farid M, Selman JR, Al-Hallaj S. Thermal conductivity enhancement of phase change materials using a graphite matrix. Appl Therm Eng 2006;26:1652–61.
[23] Alrashdan A, Mayyas AT, Al-Hallaj S. Thermo-mechanical behaviors of the expanded graphite-phase change material matrix used for thermal management of Li-ion battery packs. J Mater Process Technol 2010;210:174–9.
[24] Lv Y, Yang X, Li X, Zhang G, Wang Z, Yang C. Experimental study on a novel battery thermal management technology based on low density polyethylene-enhanced composite phase change materials coupled with low fins. Appl Energy 2016;178:376–82.
[25] Wu W, Yang X, Zhang G, Ke X, Wang Z, Situ W, et al. An experimental study of thermal management system using copper mesh-enhanced composite phase change materials for power battery pack. Energy 2016;113:909–16.
[26] Ling ZY, Wang FX, Fang XM, Gao XN, Zhang ZG. A hybrid thermal management system for lithium ion batteries combining phase change materials with forced-air cooling. Appl Energy 2015;148:403–9.
[27] Tiari S, Qiu S, Mahdavi M. Discharging process of a finned heat pipe–assisted thermal energy storage system with high temperature phase change material. Energy Convers Manage 2016;118:426–37.
[28] Tiari S, Qiu S, Mahdavi M. Numerical study of finned heat pipe-assisted thermal energy storage system with high temperature phase change material. Energy Convers Manage 2015;89:833–42.
[29] Lin Z, Wang S, Huo J, Hu Y, Chen J, Zhang W, et al. Heat transfer characteristics and LED heat sink application of aluminum plate oscillating heat pipes. Appl Therm Eng 2011;31:2221–9.
[30] Naghavi M, Ong K, Mehrali M, Badruddin I, Metselaar H. A state-of-the-art review on hybrid heat pipe latent heat storage systems. Energy Convers Manage 2015;105:1178–204.
[31] Naghavi M, Ong K, Badruddin I, Mehrali M, Silakhori M, Metselaar H. Theoretical model of an evacuated tube heat pipe solar collector integrated with phase change material. Energy 2015;91:911–24.
[32] Robak CW, Bergman TL, Faghri A. Enhancement of latent heat energy storage using embedded heat pipes. Int J Heat Mass Transf 2011;54:3476–84.
[33] Rao ZH, Wang SF, Wu MC, Lin ZR, Li FH. Experimental investigation on thermal management of electric vehicle battery with heat pipe. Energy Convers Manage 2013;65:92–7.
[34] Tran T-H, Harmand S, Desmet B, Filangi S. Experimental investigation on the feasibility of heat pipe cooling for HEV/EV lithium-ion battery. Appl Therm Eng 2014;63:551–8.
[35] Zhao R, Gu J, Liu J. An experimental study of heat pipe thermal management system with wet cooling method for lithium ion batteries. J Power Sources 2015;273:1089–97.
[36] Wang Q, Jiang B, Xue Q, Sun H, Li B, Zou H, et al. Experimental investigation on EV battery cooling and heating by heat pipes. Appl Therm Eng 2015;88:54–60.
[37] Ye Y, Shi Y, Saw LH, Tay AA. Performance assessment and optimization of a heat pipe thermal management system for fast charging lithium ion battery packs. Int J Heat Mass Transf 2016;92:893–903.
[38] Tran T-H, Harmand S, Sahut B. Experimental investigation on heat pipe cooling for hybrid electric vehicle and electric vehicle lithium-ion battery. J Power Sources 2014;265:262–72.
[39] Zou H, Wang W, Zhang G, Qin F, Tian C, Yan Y. Experimental investigation on an integrated thermal management system with heat pipe heat exchanger for electric vehicle. Energy Convers Manage 2016;118:88–95.
[40] Greco A, Cao D, Jiang X, Yang H. A theoretical and computational study of lithium-ion battery thermal management for electric vehicles using heat pipes. J Power Sources 2014;257:344–55.
[41] Ye Y, Saw LH, Shi Y, Tay AA. Numerical analyses on optimizing a heat pipe thermal management system for lithium-ion batteries during fast charging. Appl Therm Eng 2015;86:281–91.
[42] Liu F, Lan F, Chen J. Dynamic thermal characteristics of heat pipe via segmented thermal resistance model for electric vehicle battery cooling. J Power Sources 2016;321:57–70.
[43] Wu M-S, Liu KH, Wang Y-Y, Wan C-C. Heat dissipation design for lithium-ion batteries. J Power Sources 2002;109:160–6.
[44] Rao Z, Huo Y, Liu X. Experimental study of an OHP-cooled thermal management system for electric vehicle power battery. Exp Therm Fluid Sci 2014;57:20–6.
[45] Wang Q, Rao Z, Huo Y, Wang S. Thermal performance of phase change material/oscillating heat pipe-based battery thermal management system. Int J Therm Sci 2016;102:9–16.
[46] Wu W, Zhang G, Ke X, Yang X, Wang Z, Liu C. Preparation and thermal conductivity enhancement of composite phase change materials for electronic thermal management. Energy Convers Manage 2015;101:278–84.
[47] S.P. Venkateshan. Mchanical measurements, New Delhi; 2008.
[48] Ameli M, Agnew B, Leung PS, Ng B, Sutcliffe C, Singh J, et al. A novel method for manufacturing sintered aluminium heat pipes (SAHP). Appl Therm Eng 2013;52:498–504.